J Plant Growth Regul (2003) 21:441–458
DOI: 10.1007/s00344-003-0006-y

J P G R
Journal of Plant Growth Regulation

Effect of Hydrotropism on Root System Development in Soybean (*Glycine max*): Growth Experiments and a Model Simulation

Daizo Tsutsumi,* Ken'ichiro Kosugi, and Takahisa Mizuyama

Division of Forest Science, Graduate School of Agriculture, Kyoto University, Oiwakecyo Kitashirakawa Sakyoku Kyoto-City, Kyoto 6068502, Japan

Abstract

To observe root system development, soybean plants (*Glycine max*) were grown in root boxes that were set horizontally to reduce the effect of gravity. Along with the root system development, the two-dimensional distribution of soil water content in the root boxes was measured continuously by the time domain reflectometry (TDR) method. Root system development and its morphological architecture were strongly affected by the positions of the water supply. It is suggested that root hydrotropism plays the dominant role in root system development. In addition to root hydrotropism, the importance of root compensatory growth is suggested. A combined model of root system development and soil water flow considering root hydrotropism and compensatory growth was used to simulate root system development and soil water flow. The morphological architecture of root systems and the distribution of soil water content obtained in the experiment were successfully explained by the model simulation. These results confirmed that root hydrotropism and compensatory growth are dominant factors in root system development under a reduced effect of gravity. The validity of the model was confirmed, and its applications for various purposes were suggested.

Key words: Root system development; Root box; Model; TDR; Coil type probe; Hydrotropism; Compensatory growth

Introduction

Root hydrotropism, that is, root elongation bending toward a source of moisture according to a water gradient, has been known empirically, and had been reported in earlier published studies (Darwin 1880; Hooker 1915). However, little attention had been paid to hydrotropism for many years, partly because some earlier workers failed to detect the occurrence of hydrotropism (Dutrochet 1824; Keith 1815). Their failures were due to their inability to control the appropriate moisture gradient, and to the counteracting effect of gravity (Takahashi 1994). Recently, experimental methods were improved and the results have been reported in some studies. Takahashi and Scott (1993) strictly

Received: 1 September 2002; accepted: 1 January 2003; Online publication: 28 April 2003
*Corresponding author; e-mail: td3@slope.dpri.kyoto-u.ac.jp

controlled the gradient of air humidity in a closed chamber and observed that the roots of pea (*Pisum sativum* L.) and corn (*Zea may* L.) grew toward moisture. Takano and others (1995) applied a water-potential gradient to the root cap of an agravitropic pea mutant *ageotropumi*, and observed that the root elongated and bent toward the side of highest water potential. From these studies, the existence of hydrotropism was confirmed and accepted as a genuine plant tropism. Together with other root tropisms (gravitropism, thigmotropism, thermotropism, and so on) root hydrotropism may ultimately contribute to establishment of the root system, by which roots avoid environmental risks such as drought conditions and support the growth and development of the whole plant. However, in all the experiments on root hydrotropism, only the elongation of an individual root was investigated. There seems to have been no studies investigating the effect of hydrotropism on the development of the entire plant root system. Although investigations included the effect of soil moisture conditions or drip irrigation on the development of the entire root system and its morphological architecture in various crop plants (Galamay and others 1992; Kono and others 1987) or vegetables (Morita and Toyoda 1998), these effects were not considered as root hydrotropism, and sufficient theoretical considerations were not carried out.

Numerical simulation using a root system development model is one of the available methods for theoretical considerations of the mechanisms of root system development. Root system development models, in which root elongation factors (that is, elongation rate, growth orientation, and branching) are described mathematically, can simulate root system development under the ground, and have been used to predict root system architecture in various plants. Root system development models can also be used for inspecting the appropriateness of the hypothesis employed in the model by comparing the simulated and observed root system morphologies. Furthermore, root system development models, combined with water or nutrient uptake models, can be used for simulating synchronized root system development and its soil water uptake or nutrient uptake behaviors. Diggle (1988) and Pages and others (1989) separately proposed fundamental models that simulate the three-dimensional growth and architecture of a root system. On the other hand, Clausnitzer and Hopmans (1994) proposed a model that combined root system development and soil water uptake. Somma and others (1998) proposed a model that combined root system development and nutrient uptake. They succeeded in simulating the three-dimensional root system development and soil water or nutrient uptake behaviors. Many models have been proposed to simulate root system development in various plant species (for example, Lynch and others 1997; Jourdan and Rey 1997; Shibusawa 1994). Although gravitropic response in root elongation was considered in all the models, the hydrotropic response of roots was generally not considered. Only in the model by Clausnitzer and Hopmans (1994) is the root hydrotropic effect considered implicitly; they assumed that roots respond to the soil strength gradient that is defined as a function of the soil moisture content. Recently, Tsutsumi and others (2001, 2003) proposed a two-dimensional root system development model considering hydrotropism explicitly, combined with a soil water uptake model. The model simulated root system development in Japanese red pine (*Pinus densiflora*) and soil water flow due to the water extraction. The simulation results demonstrated plagiogravitropic elongation of lateral roots and the asymmetric architecture of root systems under slope conditions (Tsutsumi and others 2001, 2003). However, because the comparison between simulated and observed root systems was not sufficient in the previous studies, the effect of hydrotropism on root system development was not confirmed clearly.

In the present study, we grew the root systems of soybean plants in root boxes with 25 coil-type probes for time domain reflectometry (TDR) measurement. We observed the two-dimensional root system architectures that developed with water supplies from different positions, and measured the two-dimensional distribution of soil water content change along with the root system development. The objective of this experiment was to investigate the effect of soil water conditions on root system development by quantitative measurements of root system morphological architecture and distribution of soil water content. Furthermore, we simulated the root system development and the soil water flow by using a model that considers hydrotropism (Tsutsumi and others 2003), and clarified the role of hydrotropism in root system development by comparing the observed and the simulated root systems. The concept of root compensatory growth was also employed in the model, and the effect of compensatory growth on root system development was investigated.

Materials and Methods

Plant Growth Experiment

Plant. Soybean plants (*Glycine max*), which have been widely used in many experimental

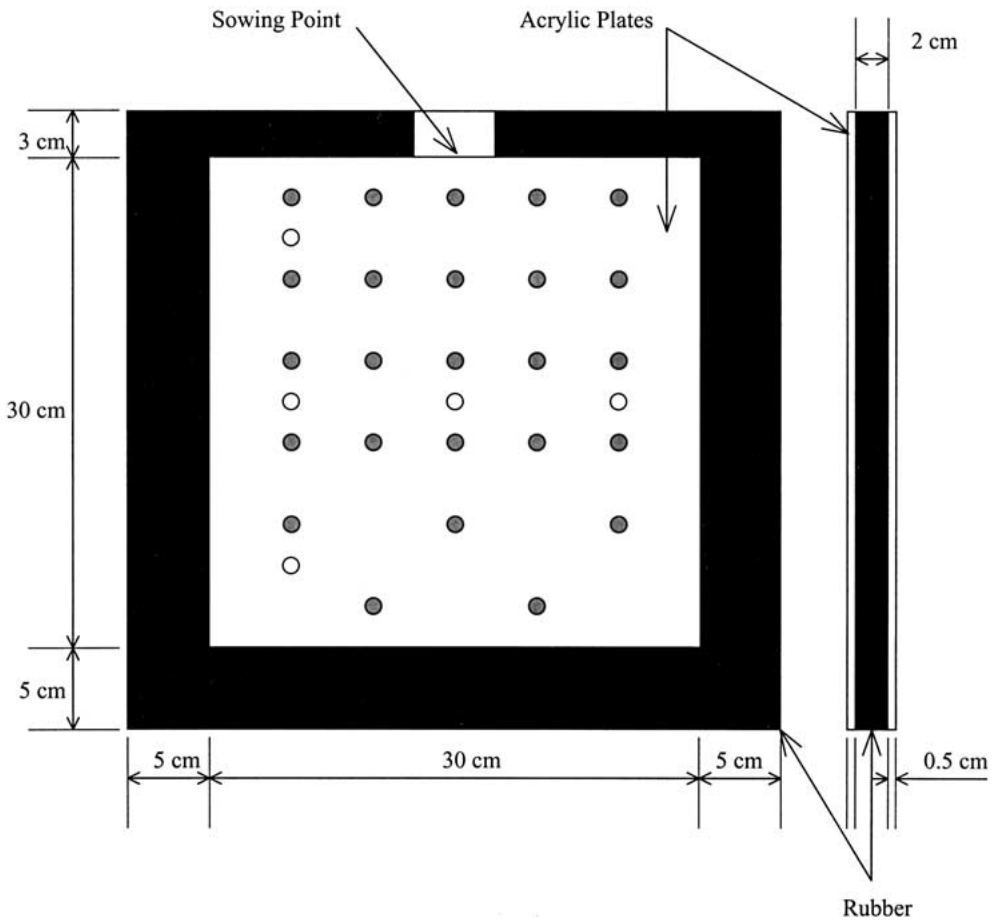

Figure 1. Front and side views of the root box (● TDR probes ○ porous cups).

studies (for example, Kono and others 1987; Lynch and van Beem 1993; Raper and Barber 1970), were used in the experiment. The root system of the soybean is generally classified into the basal root system category, which is similar to a main root system, and shows relatively simple morphology when compared to a fibrous root system, which typically is seen in cereal plants such as wheat, corn or rice.

Root box. Four root boxes (30 cm in width and length, 2 cm in thickness) were made according to Kono and others (1987). The TDR probes were installed in two of them, root box No. 1 and No. 2. The front and side views of the root box are shown in Figure 1. Gray circles in Figure 1 indicate the points where the TDR probes described below were installed (Root box No. 1 and No. 2). White circles indicate the points where porous cups were installed (horizontal 3 circles in the middle for root box No. 1 and No. 3, and vertical 3 circles on the left for root box No. 2 and No. 4). We used the porous ceramic cups that are usually used as tensiometers. Figure 2 shows a sectional view of a porous cup that is installed into the root box. The water supply system to the root boxes is shown in Figure 3. The porous cups were connected to the water tanks by tubes, and the water was continuously supplied from these porous cups. The water tanks were placed 25 cm lower than the root boxes, so that the water potential inside the porous cups was controlled at −25 cm. The rate of water supply changes according to the differences in the water potential between the porous cups and soil, and the hydraulic conductivity of porous material. Using root boxes for root growth experiments is advantageous in preserving the root system for observation without any impairment or disturbance of its structure (Kono and others 1987).

TDR probe. TDR probes (coil-type) were installed in the root box (see Figure 1), so that the two-dimensional distribution of soil water content could be measured during root growth. The details of the coil-type TDR probe are shown in Figure 4. The probe was designed to fit the thickness of the root box, and manufactured in accordance with recent studies (Nissen and others 1998; Vaz and Hopmans

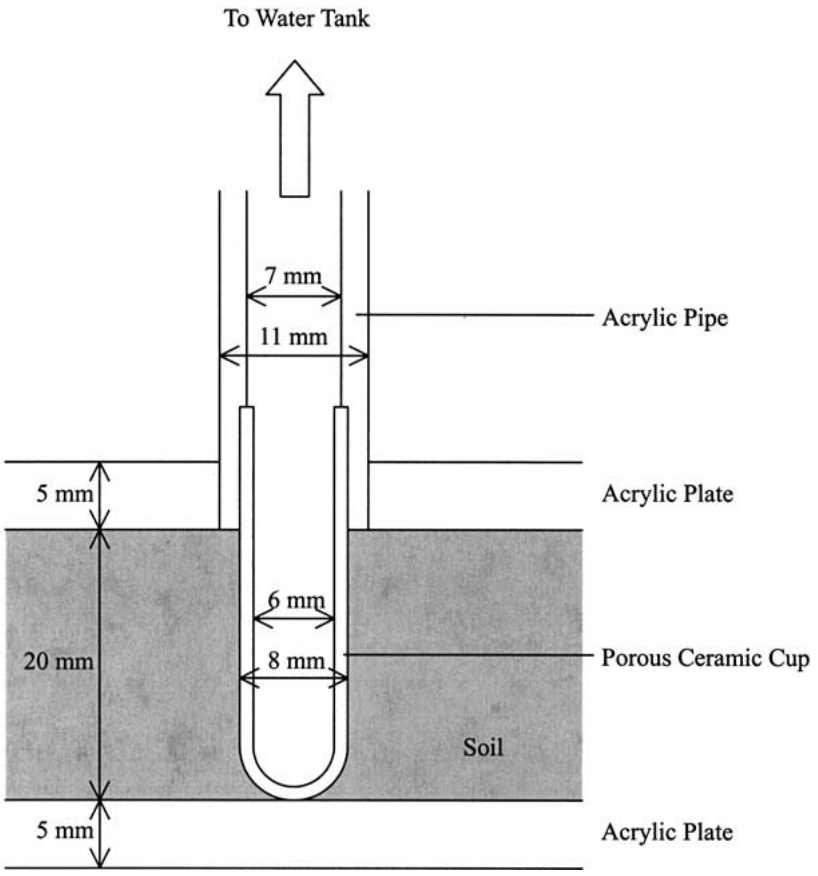

Figure 2. A sectional view of a porous cup, and its installation in the root box.

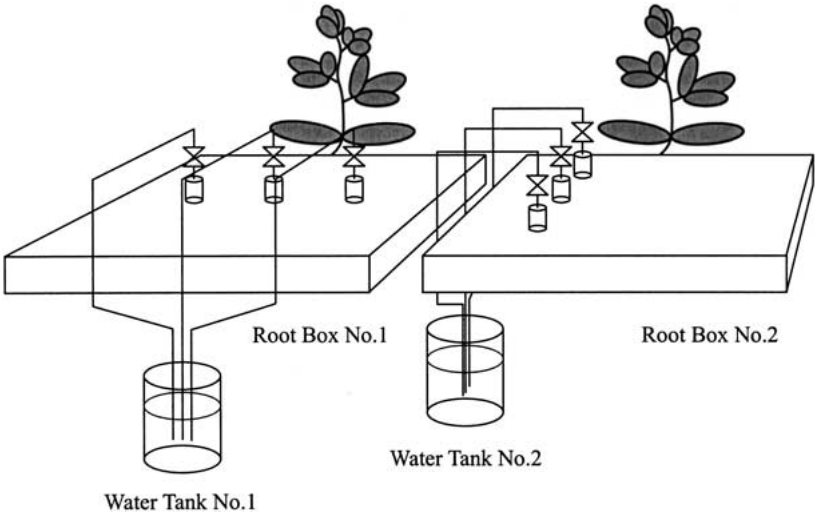

Figure 3. A water supply system to the root boxes; root boxes, porous cups, tubes, and water tanks (the water tanks were set 25 cm lower than the root boxes, so that the water potential inside of the porous cups was controlled at −25 cm. The root boxes were set horizontally, after germination, on the 8th day after sowing.).

2001). The probe consisted of two stainless steel wires coiled around an acrylic pipe. The coil length was less than 2.0 cm, so that it fit within the depth of the root box. Therefore, the interval of the coil was about 1.7 mm. The stainless steel wires were connected to the coaxial cable inside the acrylic pipe. Inside the pipe, the wires were sleeved by silicon tubes to prevent a short-circuit. Furthermore, the acrylic pipe was filled with silicon sealant to prevent soil water from leaking into the pipe

For the TDR measurement, the TDR100 equipment (Campbell Scientific Inc, Utah, USA) was used. Prior to the plant growth experiments, the

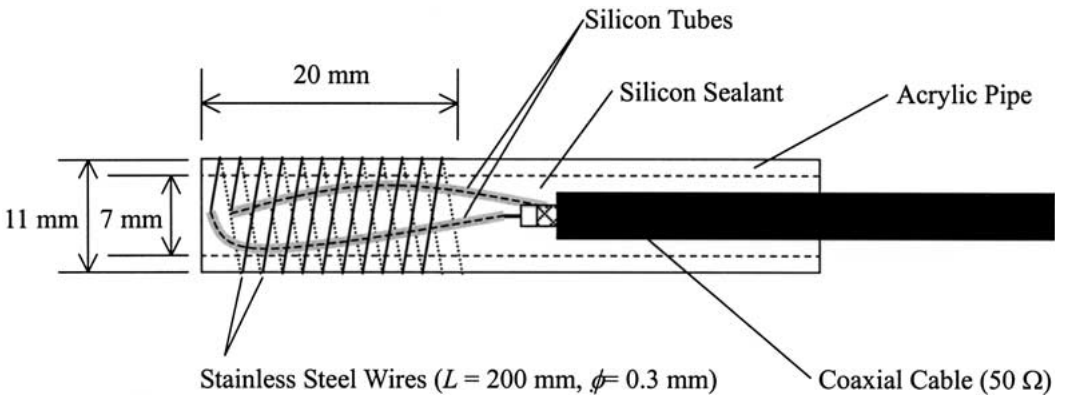

Figure 4. Detail of a coil-type TDR probe. (The stainless steel wires were coiled around the acrylic pipe, and connected to the coaxial cable inside of the pipe.)

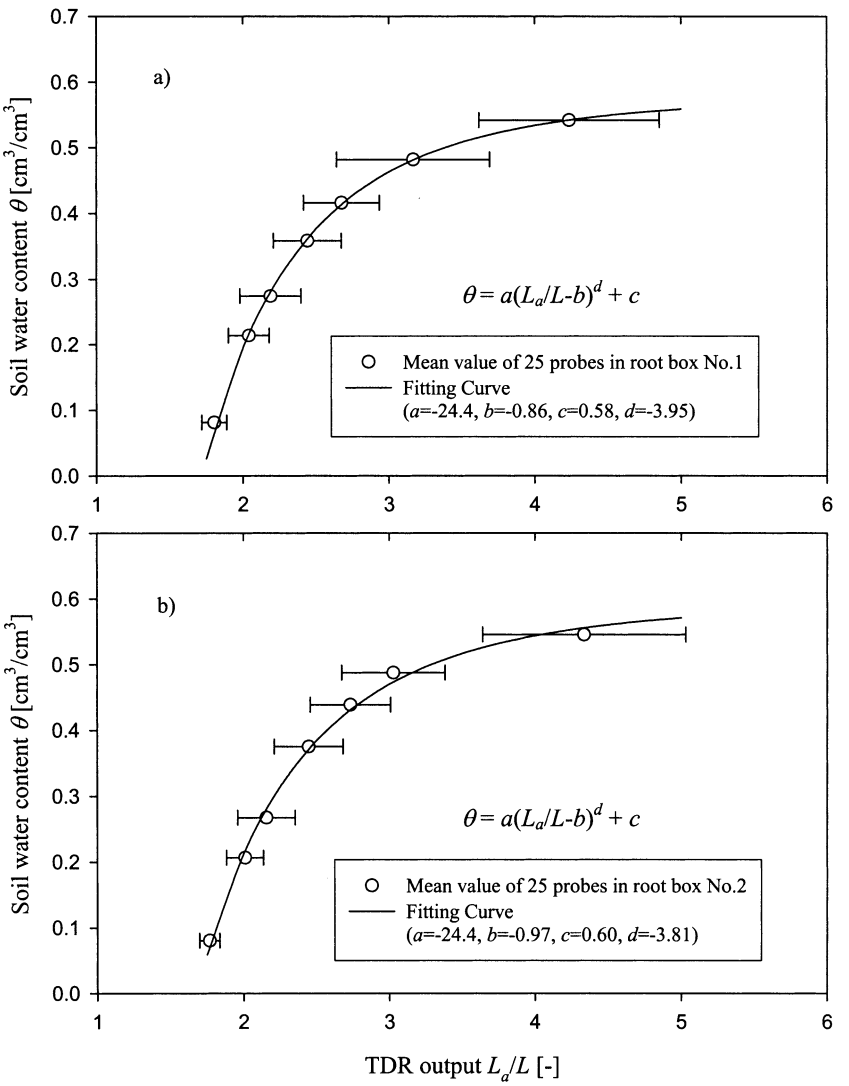

Figure 5. Coil-type TDR probe calibrations in root box (a) No. l and (b) No. 2. (Measured relationship L_a/L–θ, and their fitting curves. Error bars indicate the standard deviations. Fitting equation and parameters are also shown in the figure.)

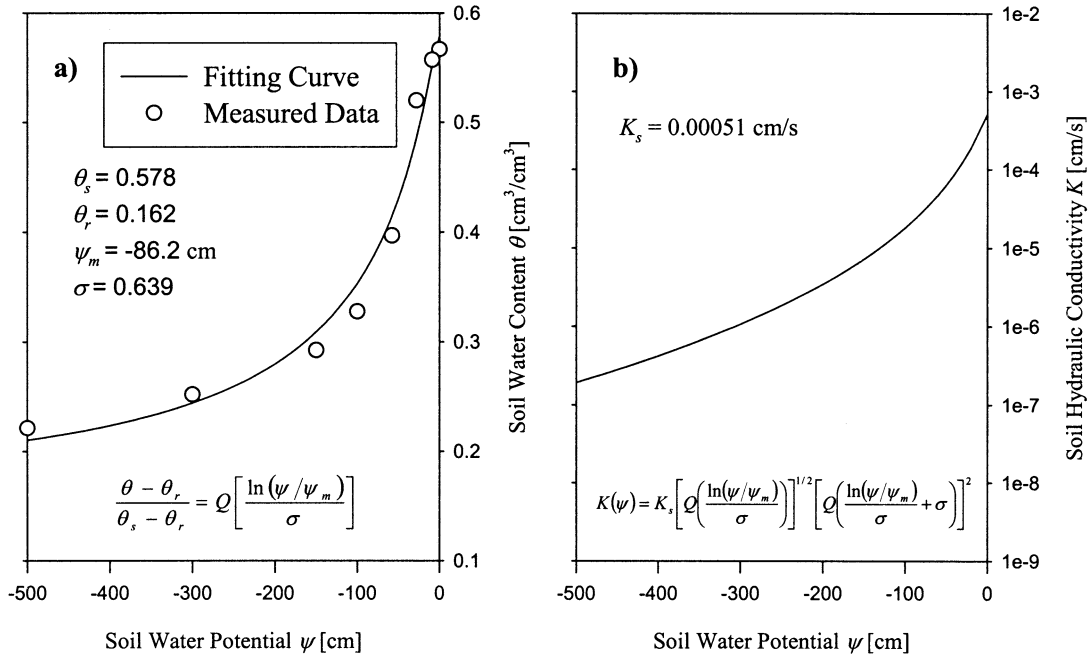

Figure 6. Hydraulic properties of soil, relationship (**a**) θ–ψ (**b**) *K*–ψ. (The equations in the figures represent the lognormal model, where function *Q* represents the residual normal distribution. The parameters for the lognormal model are also shown in the figure.)

TDR probes in the root boxes were calibrated. The calibration curves of the TDR probe in each root box are shown in Figure 5. Circles in Figure 5 indicate the average values of the 25 probes in root box No. 1 and 2, and error bars indicate the standard deviations. The fitting equation and its parameters are also shown in Figure 5. These curves were used for the calculation of the soil water content in root boxes. Further consideration for the TDR calibration was made elsewhere (Tsutsumi and others 2002).

Soil. A sandy soil excavated at Kamigamo Experimental Forest of Kyoto University (Kyoto City, Japan) and an organic soil were mixed (50:50 vol.%) for the experiment. The soil was fertilized with 3.0 g of granular fertilizer (N, 6%; P, 40%; K, 6%; Mg, 15%) per 1 kg of the soil. The initial soil water content θ [cm^3/cm^3] was set at 0.20 cm^3/cm^3, and then the root boxes were filled with the soil with a controlled bulk density of 1.07 g/cm^3. The observed retention curve of the soil is shown in Figure 6, together with soil hydraulic conductivity represented by the lognormal model proposed by Kosugi (1996). The parameters for the lognormal model were determined based on the observed retention curve (Figure 6).

Experiment. Experiments were carried out in a green house at the Experimental Forest of Kyoto University (Kyoto City, Japan) from April 27th to May 28th, 2002. The highest, lowest, and average temperatures in the green house during the experiment were 42.9, 10.2, and 22.3°C, respectively. In the beginning of the experiment, seeds were sown on the top of each root box which were set vertically until germination (7th day after sowing), then were set horizontally after germination, so that the effect of gravity on both root elongation and soil water flow could be reduced (see Figure 3).

The TDR measurement and water supply were started after germination. The interval of TDR measurements was 10 minutes, and water was continuously supplied from the porous cups. Covering the soil surface prevented evaporation. During the experiment, the amount of supplied water and total weight of the root boxes were measured once a day at 18:00 so that the amount of daily transpiration could be determined. At the end of the experiment, the root boxes were broken apart and the soil was removed carefully so as not to disturb the root systems. Photographs were taken to record the architecture of the root systems. The characteristics of the root architecture (that is, branching interval, root length, maximum branching order) were measured so they could be used in the model simulation.

Root System Development Model

Root elongation. The authors previously proposed a combined model of the two-dimensional root sys-

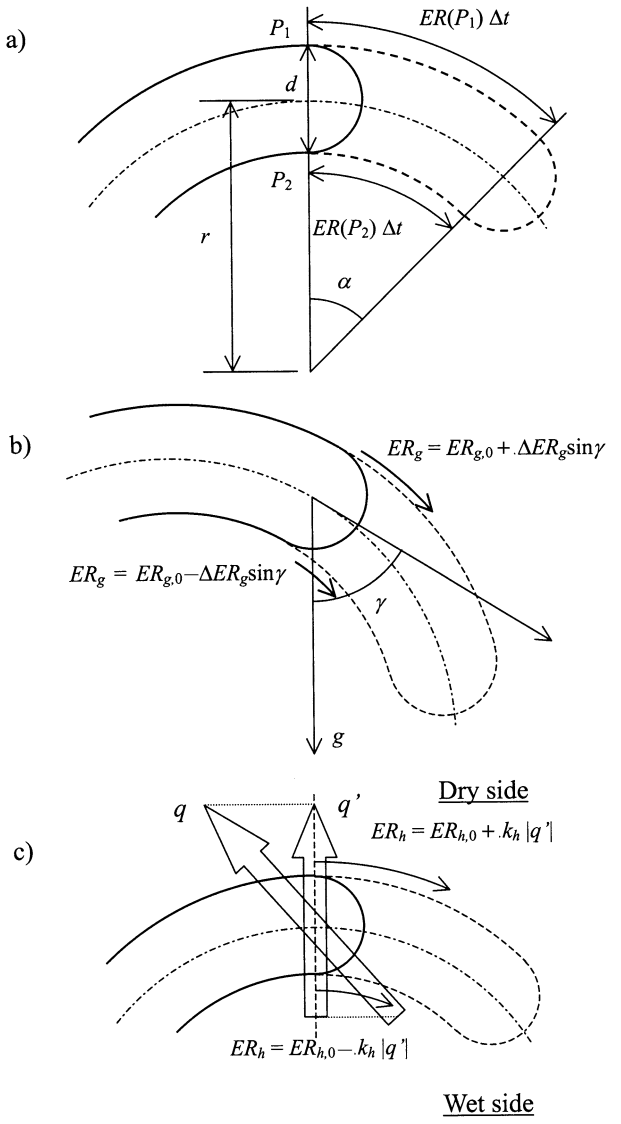

Figure 7. Model principles of root elongation; (**a**) mechanism of differential growth, (**b**) gravitropic response, (**c**) hydrotropic response of root.

tem development and water uptake (Tsutsumi and others 2003). In the proposed model, root hydrotropism was considered specifically and root elongation was expressed by differential growth, which is regarded as a mechanism of actual root elongation (Ishikawa and others 1991; Takahashi 1994). Figure 7a shows the mechanism of root differential growth. As shown in the figure, root elongation (that is, angle A [rad] and radius r [cm]) is determined by root diameter d [cm] and the elongation rate ER [cm/s] in each elongation point of the root (that is, P_1 and P_2), as follows:

$$r = \left|\frac{ER(P_1) + ER(P_2)}{ER(P_1) - ER(P_2)}\right| \frac{d}{2} \tag{1}$$

$$\alpha = \frac{|ER(P_1) - ER(P_2)|}{d} \Delta t \tag{2}$$

where, Δt [s] is a time step. Also, the elongation rate of the center of the root, ER_c [cm/s], can be expressed as follows:

$$ER_c = \frac{ER(P_1) + ER(P_2)}{2} \tag{3}$$

In the model, ER is computed as the sum of the gravitropic elongation rate, ER_g [cm/s], and hydrotropic elongation rate, ER_h [cm/s]:

$$ER = ER_g + ER_h \tag{4}$$

The function of the gravitropic elongation rate was defined as (see Figure 7b):

For the upper side elongation point:

$$ER_g = ER_{g,0} + \Delta ER_g \sin\gamma \quad 0 \le \gamma \le \pi/2 \tag{5}$$

$$ER_g = ER_{g,0} + \Delta ER_g \quad \pi/2 \le \gamma \le \pi \tag{6}$$

For the lower side elongation point:

$$ER_g = ER_{g,0} - \Delta ER_g \sin\gamma \quad 0 \le \gamma \le \pi/2 \tag{7}$$

$$ER_g = ER_{g,0} - \Delta ER_g \quad \pi/2 \le \gamma \le \pi \tag{8}$$

where, γ [rad] is the angle between the directions of gravity and root orientation, $ER_g,0$ [cm/s] gives the value of the gravitropic elongation rate when the root directs toward gravity (γ= 0); ΔER_g [cm/s] is the constant that determines the intensity of gravitropism. The function of hydrotropic elongation rate was defined as (see Figure 7c):

Wet side

$$ER_h = ER_{h,0} - k_h|q'| \tag{9}$$

Dry side

$$ER_h = ER_{h,0} + k_h|q'| \tag{10}$$

where, $|q'|$ [cm/s] is the magnitude of the component of water flux q [cm/s], perpendicular to the root at the root cap, $ER_h,0$ [cm/s] gives the value of the hydrotropic elongation rate when $|q'| = 0$, k_h [−] is the parameter that determines the intensity of hydrotropism. The water flux q can be obtained from the simulation of soil water flow calculated by the finite element method. From Equations 3–10, ER_c can be expressed as

$$ER_c = ER_{g,0} + ER_{h,0} \tag{11}$$

In obtaining ER from Equation [4-10], it is not necessary to divide ER_c into $ER_g,0$ and $ER_h,0$. The measured value of ER_c was given for the simulation.

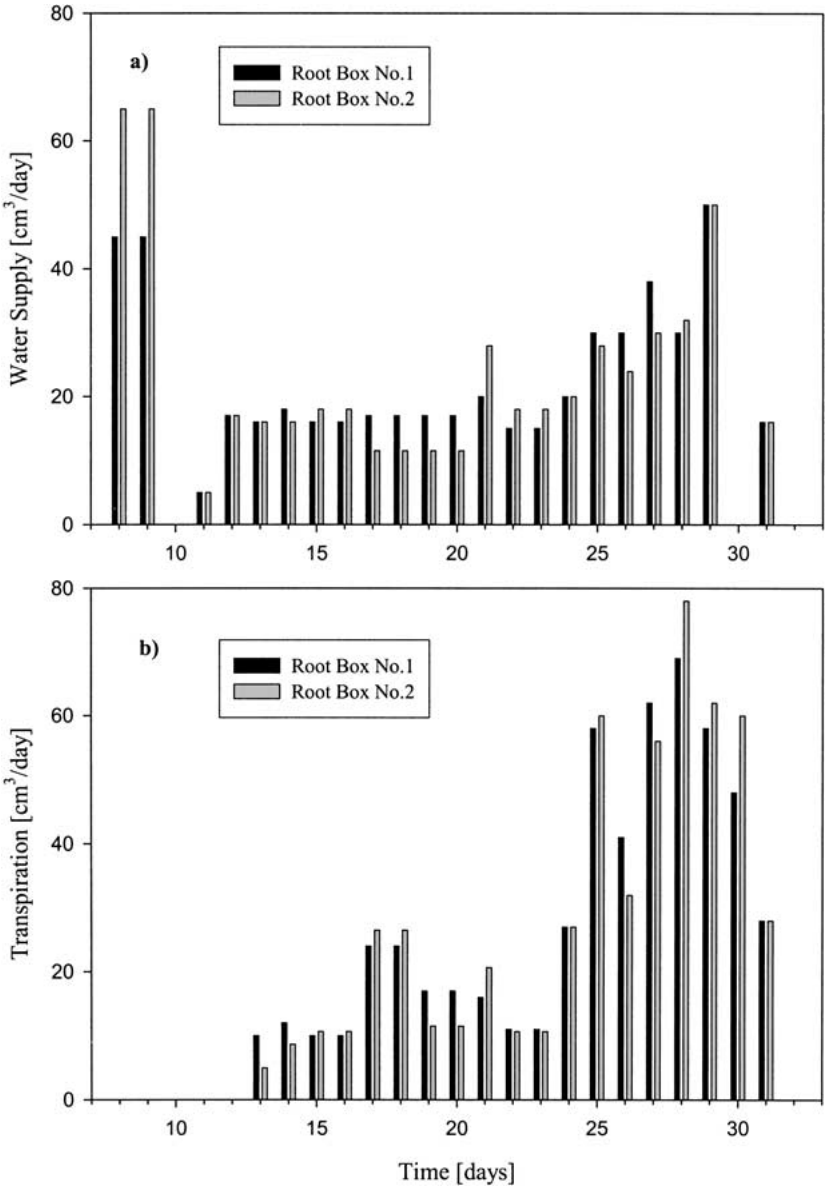

Figure 8. Changes of (**a**) amount of water supply, and (**b**) daily transpiration measured in the experiment. (Data are also used for the model simulation.)

In the previously proposed model (Tsutsumi and others 2003), we assumed that k_h is a constant. However, to simulate the root system morphology obtained by the experiment, we assumed that k_h is a decreasing function of the soil water potential ψ [cm] at the root tip. The function k_h was defined as follows:

$$k_h = a_h(\psi - \psi_h) \quad \psi < \psi_h \tag{12-1}$$

$$k_h = 0 \quad \psi_h \cdot \psi \tag{12-2}$$

where, a_h [cm^{-1}] is a coefficient that has a negative value and ψ_h [cm] is a threshold value of water potential that has a negative value. By this definition, the root hydrotropic response becomes stronger under drought conditions, and the root does not show hydrotropism under moist condition where ψ is higher than ψ_h. From the physiological point of view, it seems to be quite natural that the root responds hydrotropically stronger under drought conditions than under a moist condition where the root can easily extract water.

Root branching. Root branching may be as important as root elongation in root system development. From the observation of actual root systems in the experiment, we confirmed main root growth as obvious and first order lateral root branching from the main root at a roughly constant interval. More than third order lateral roots were negligible. We therefore assumed the soybean root system to be a main root system, and dealt with the main root and less than second order lateral roots in the model. For simplic-

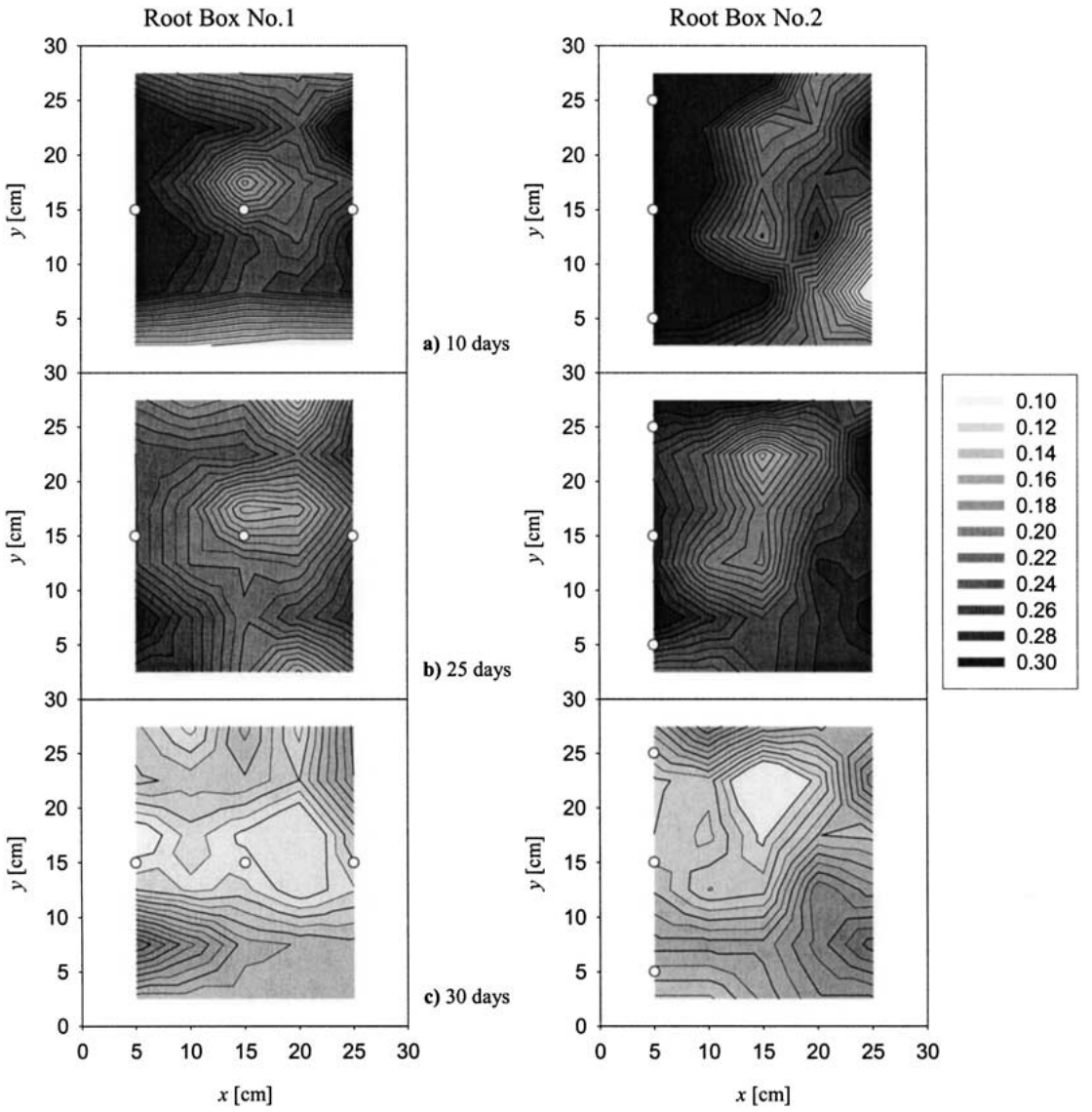

Figure 9. Changes in the distribution of soil water content θ [cm^3/cm^3] in root box No. 1 and No. 2, measured by the TDR method in the experiment. (White circles indicate the points of water supply.)

ity, we assumed a constant branching interval. The details of the branching parameters are in accordance with the model proposed by Pages (Pages and others 1989) and described in Tsutsumi and others (2003).

Soil water flow. This was calculated according to the two-dimensional Richards' equation based upon water potential. The soil water capacity and hydraulic conductivity in the Richards' equation were represented according to the lognormal model proposed by Kosugi (1996, Figure 6). In the simulations, we employed the Richards' equation assuming *x–z* coordinate, and considered root gravitropism during the time root boxes were set vertically (until the 7th day after sowing). During the time root boxes were set horizontally (from the 8th day after sowing), we employed the Richards' equation assuming *x-y* coordinate, and did not consider root gravitropism. Water extraction by the root system was determined according to the model of Herkelrath and others (1977) and Kanda and Hino (1990) as follows:

$$S = -\left(\frac{\theta - \theta_r}{\theta_s}\right)^b \rho \Delta\psi L \qquad (13)$$

$$\Delta\psi = \psi_c + R_c l - \psi \qquad (14)$$

where, S [s^{-1}] is the water extraction intensity, θ [cm^3/cm^3] is the soil water content at the root surface, ρ [s^{-1}] is the water penetration coefficient

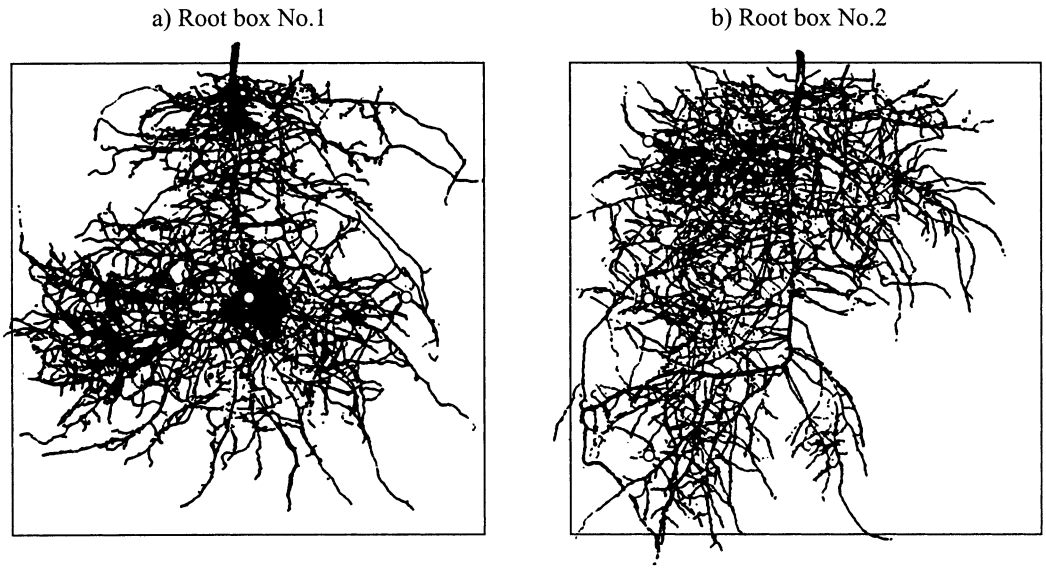

Figure 10. Observed root system architectures from (**a**) root box No. 1 and (**b**) No. 2. (White circles indicate the points of water supply, and the squares indicate the boundary of the root boxes 30 × 30 cm.)

of the root, b [−] is a correction parameter, $\Delta\psi$ [cm] is the difference of the water potential between root and soil, L [cm/cm^2] is the root length density, ψ_c [cm] is the water potential of the beginning point of the main root, l [cm] is the distance from the beginning point of the main root to the root and R_c [-] is a correction coefficient for the friction loss of water transport in the root. We assumed that the length of roots whose age does not exceed 10 days is counted in L, and contributes to soil water extraction. The equations for soil water flow were solved numerically by the partially implicit finite element method (Istoke 1989; Zienkiewicz 1971). The detailed methods for these calculations were reported in Tsutsumi and others (2003). To simulate root system development and soil water flow in the root box experiment, we used the observed data for the actual daily amount of water supply and transpiration. In the model calculation we assumed that the transpiration rate changed according to a sine curve during the daytime, and the water was supplied equally to three porous cups at a constant rate during a day.

Results of Experiment

Water Supply and Daily Transpiration

Figure 8a shows the amount of water that was supplied to the root boxes from the porous cups, and Figure 8b shows the amount of daily transpiration. Figure 9 shows the distribution of soil water content θ at 15:00 in root box No. 1 and 2, obtained by the TDR measurements. Until the 7th day after sowing, the amount of water supplied was zero because the porous cups were not connected to the water tanks. Just after the porous cups were connected to the water tanks (the 8th day after sowing), a large amount of water was supplied to the root boxes because the soil water conditions were relatively dry (averaged water content was 0.20 cm^3/cm^3), and the water supply rapidly decreased because the soil then became relatively moist (averaged water content was 0.25 cm^3/cm^3 in the root box No. 1 and 0.28 cm^3/cm^3 in the root box No. 2). From the water supply, the soil near the porous cups became moist (see Figure 9a). At this stage of the experiment, transpiration did not occur because the plants had not grown enough (Figure 8b).

From the 13th day after sowing, transpiration began, and a roughly constant amount of water was supplied from the 12th through the 24th day after sowing. From the 24th day after sowing, transpiration increased along with plant growth, and the amount of water supply increased from the 25th day after sowing. The increasing transpiration caused drought areas in the soil in the root boxes (see Figure 9b). From 18:00 on the 29th day after sowing to 21:00 on the 30th day after sowing, water supplied to the root box was stopped in order to measure the soil water distribution in the case of zero water supply. Due to this condition, the soil became drier and the drought area increased (see Figure 9c). The transpiration and amount of water supply decreased during the last few days. Comparing the amount of water supplied and transpi-

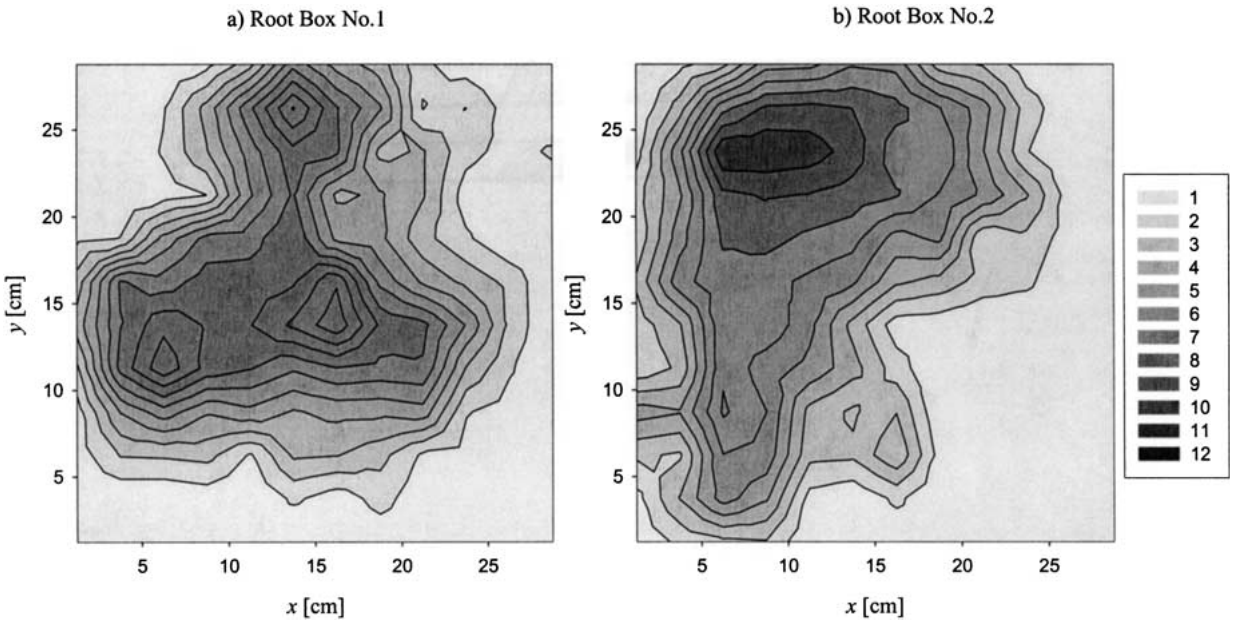

Figure 11. Distribution of the root length density [cm/cm^2] in the root box (**a**) No. 1 and (**b**) No. 2, measured by image analyzing software. The concentration of the root length can be seen. (The figures correspond to the root systems shown in Figure 10.)

ration between root boxes, the difference was small. On the other hand, the distribution of soil water content was different between the root boxes due to the differences in root system distributions and the position of the water supply.

Observed Root System Architecture

Figure 10a, b shows the observed root system architecture that developed in root box No. 1 and 2. White circles indicate the position of the porous cups from which water was supplied. In Figure 10a, b, the two root systems show different morphologies and it is obvious that the root system development was affected by the water supply. The root hydrotropic responses were especially clear in Figure 10b where the main root suddenly deflected left, in the direction of the water supply, and some of the lateral roots in the right side region were in a transition of their orientation from right to left. During the growth experiment, we observed that the main root grew straight when the root box was set vertically (until the 7th day after sowing), and then began to deflect just after the root box was set horizontally and the water supply was started (from the 8th day after sowing). Consequently, it is clear that the sudden deflection of the main root seen in Figure 10b is a result of the hydrotropic response toward the source of water under the reduced effect of gravity. By the root hydrotropic responses, the roots concentrated around the points of water supply. A similar concentration of roots can also be seen in Figure 10a. In addition to the effect of hydrotropism, an increased root elongation rate in a relatively moist area also seemed to cause root concentration. In Figure 10a, roots in the central region, near the points of water supply, grew relatively longer than the roots near the surface, which had derived earlier than those in the central region. This increase in the root elongation rate in a favorable environment is called ''compensatory growth'', and was reported in an earlier study (Crossett and others 1975). As a result, we conclude that root system development and its morphological architecture as shown in Figure 10a, b were affected by both root hydrotropism and compensatory growth.

To quantitatively estimate root morphological architecture, especially the concentration of roots, we divided each square (30 × 30 cm) shown in Figure 10a, b into 144 sub-squares (2.5 × 2.5 cm) by lines parallel to the x and y axis, and then measured the root length [cm] in each sub-square by using image analyzing software (Scion Image, Scion Co., USA.). The root length density [cm/cm^2] was obtained by dividing the measured root length by the area of the sub-square. The distribution of root length density is shown in Figure 11. We can see that Figure 11 accurately reflects the actual root system architectures and the concentration of roots

Table 1. Parameters for Model Simulation

Parameters [unit]	Main root	1st Order lateral root	2nd Order lateral root
ER_c [cm/day]	$2.77(1-t/t_{max})^{1.345}$	0.59 (long type) 0.17 (short type)	0.34
$\Delta ER_g/ER_c$ [-]	0.0004	0.0001	0.0001
a_h [-]	−2.5	−2.5	−2.5
ψ_h [-]	−60	−60	−60
a_e [-]	4.0	4.0	4.0
ψ_e [-]	−250	−250	−250
Apical non-branching zone [cm]	5.25	3.55	—
Basal non-branched zone [cm]	0.245	0.370	—
Branching interval [cm]	—	0.245	0.370
Insertion angle [degree]	—	90	90
b [-]*	1	1	1
ρ [s^{-1}]*	$1.0*10^{-9}$	$1.0*10^{-9}$	$1.0*10^{-9}$
R_c [-]*	0.05	0.05	0.05

According to aHerkelrath and others (1977), aKanda and Hino (1990).

shown in Figure 10. By collating the distribution of root length density as shown in Figure 11 and the distribution of soil water content as shown in Figure 9c, the root concentrated area and the soil drought area are in good agreement. It is therefore obvious that the soil water was extracted dynamically in the root concentrated area. The observed total root lengths were 26.3 m in root box 1 and 26.0 m in root box 2. From these similar values, the root systems grew equally in spite of the different positions of water supply. These quantitative estimations of root length density can be used to compare the root system morphologies obtained by model simulation.

Results of Simulation

Taking Experimental Results into Model Simulation

All the parameters used for the model simulation are shown in Table 1. From the observation and measurement of the root systems, we obtained the root elongation rate. We classified first order lateral roots into two types, that is, long type and short type, and gave the different elongation rates for each type (see Table 1). The frequencies of long and short type first order lateral roots were 33% and 67%, respectively. We also observed that the elongation rate of the main root changed during the experiment, so we defined the elongation rate of the main root as a function of time (see Table 1). ΔER_g, a_h, and ψ_h were determined by trial and error calculations, so that the model would simulate root systems similar to the actual root systems observed in the experiment. To take into account the compensatory growth of the root system that we observed, we introduced a new function, root elongation activity A_e [-] as follows:

$$A_e = 0 \quad \psi \le \psi_e \tag{15-1}$$

$$A_e = a_e(\psi - \psi_e) \quad \psi_e < \psi \tag{15-2}$$

where, a_e [-] is a coefficient that has a positive value, and ψ_e [cm] is a threshold value of water potential that has a negative value. By multiplying A_e to the elongation rate ER_c, the root grows faster in moist areas and stops growing in areas where the soil water potential ψ is lower than ψ_e. To keep the total root length independent from the root elongation activity A_e, we defined root elongation rate considering the root elongation activity, ER_c'[cm/h], as follows:

$$ER_c' = \frac{\sum_n ER_c}{\sum_n A_e ER_c} A_e ER_c \tag{16}$$

where, n [-] is the root number. By this definition, the total root length will be preserved in each simulation. Instead of ER_c, ER_c' was used for obtaining ER in Equation [4]. a_e and ψ_e were determined by trial and error calculation, so that the model would simulate the root systems similar to the actual root systems observed in the experiment. Branching parameters, that is, apical non-branching zone

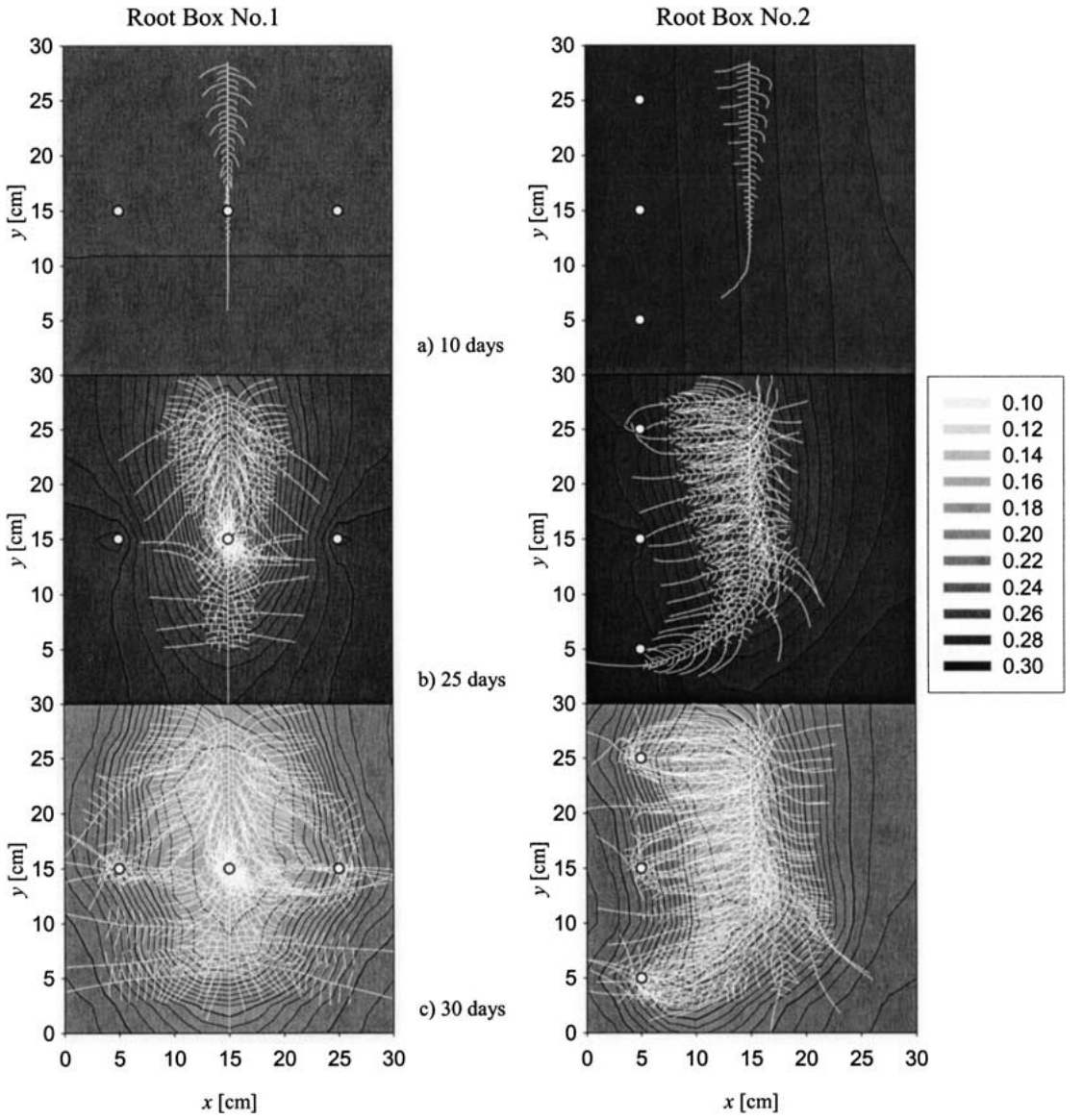

Figure 12. Simulated root system development and distribution of soil water content θ [cm^3/cm^3] in the root boxes. (Hydrotropism and compensatory growth are included. White circles indicate the points of water supply.)

[cm], basal non-branched zone [cm], branching interval [cm], and insertion angle [degree] (Pages and others 1989; Tsutsumi and others 2003) were obtained by measurement of the actual root system. Parameters for the water extraction, that is, b, ρ, and R_c, were determined according to Herkelrath and others (1977) and Kanda and Hino (1990).

Simulated Root System and Distribution of Soil Water Content

Figure 12 shows the simulated root system development and distribution of soil water content θ in root box No. 1 and 2 at 15:00, at each of the three different stages of the simulations, corresponding in time to those shown in Figure 9. On the 10th day after sowing, the main root grew straight in root box No. 1. On the other hand, it began to deflect toward the direction of the water supply in root box No. 2. This deflection was similarly seen in the actual root system development in root box No. 2, as mentioned above. The distribution of soil water content caused by the water supply can be seen in both root boxes. On the 25th day after sowing, root systems grew larger and many lateral roots elongated toward the porous cups. Because of soil water extraction by roots, drought areas appeared in both root boxes. On the 30th day after sowing, the soils became drier and their areas corresponded to the root distribution. The concentrations of the roots to the points of

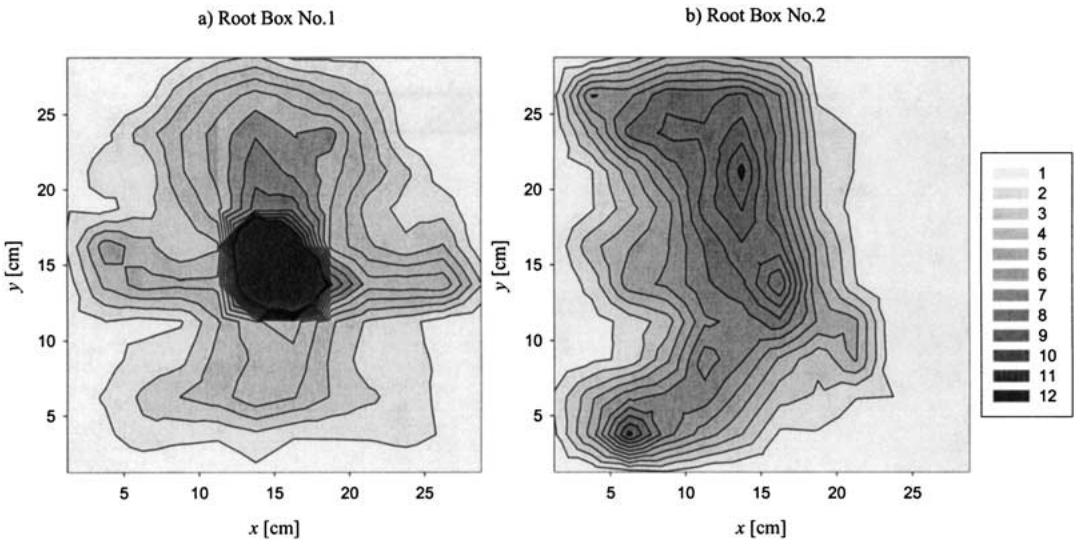

Figure 13. Simulated distribution of root length density [cm/cm^2] in the root box (**a**) No. 1 and (b) No. 2. The concentrations of the root lengths can be seen. (The figures correspond to the root systems shown in Figure 12c.)

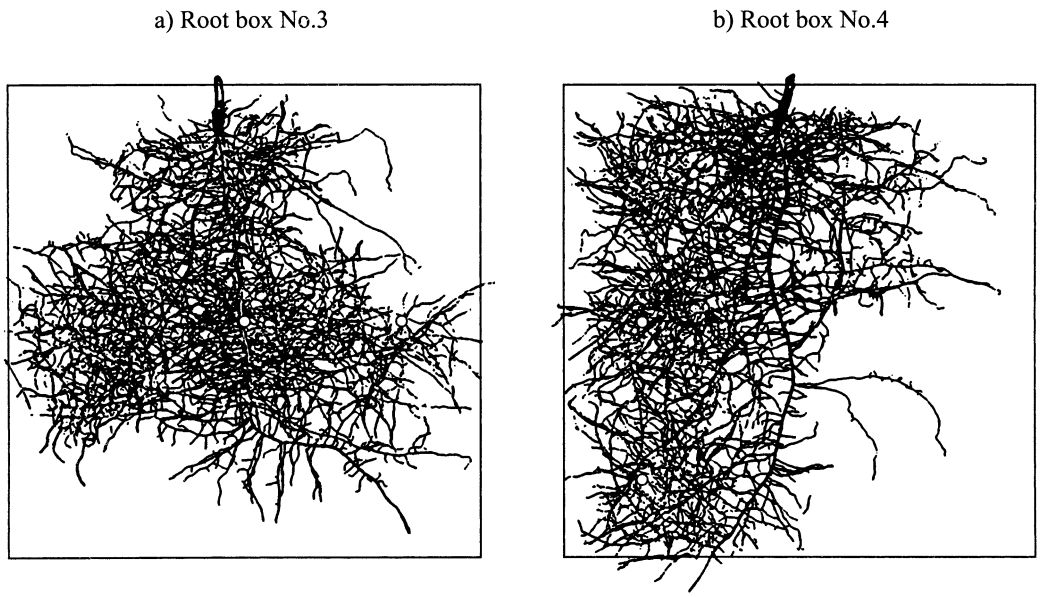

Figure 14. Observed root system architectures developed in the root box (**a**) No. 3, and (**b**) No. 4, without the TDR measurement. (White circles indicate the points of water supply, and the squares indicate the boundary of the root boxes 30 × 30 cm.)

water supply can be seen in both root boxes, similar to the actual root systems (see Figure 10). In both root systems, not all roots elongated toward the points of water supply. There were some roots elongating in a direction away from the points of water supply (for example, lower part in root box No. 1, and right lower part in root box No. 2). This elongation may be explained as follows. At the later stage of the growth period, the soil area corresponding to the root system became drier due to transpiration, and the moisture content was not evenly distributed. As a result, there appeared wetter areas far from the points of water supply. Therefore, some roots in the wetter parts of the root box responded hydrotropically in a direction away from the points of the water supply. Similar root elongation and soil water distribution can be seen in the experimental results in Figures 9 and 10. In-

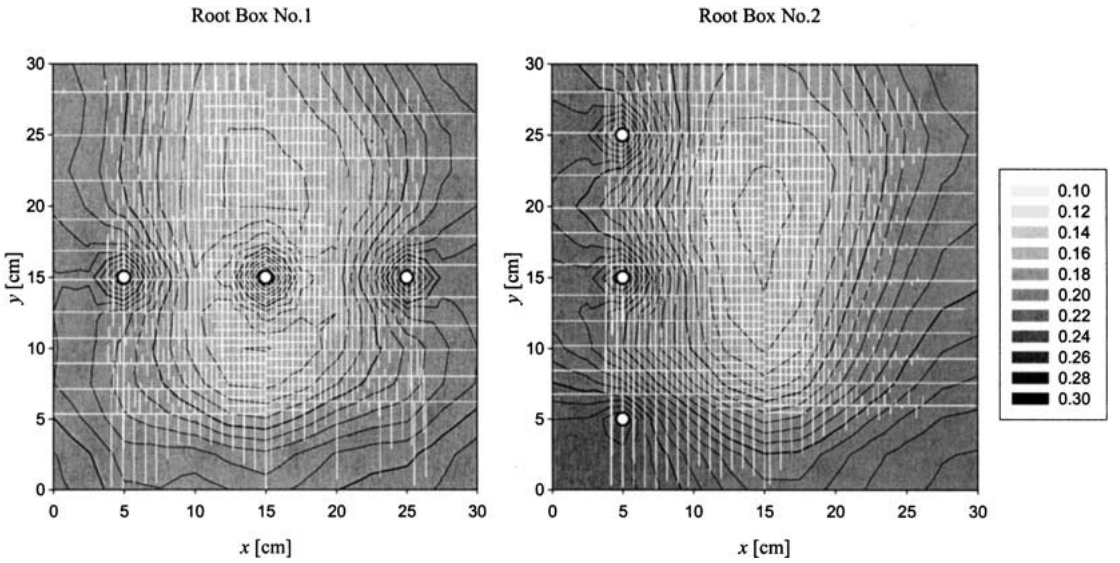

Figure 15. Root system architectures and distributions of soil water content in the root box (**a**) No. 1, and (**b**) No. 2, simulated with the effect of compensatory growth and without the effect of hydrotropism. The root grew straight, and obvious concentrations of roots cannot be seen.

cluding these root elongations, the morphological architectures of the simulated root systems are in good agreement with those of the actual root systems observed in the experiment. Moreover, the simulated total root length was 24.6 m in both root boxes, close to the actual measured total root length 26.3 m in root box No.1 and 26.0 m in root box No. 2. This would indicate that ER_c was appropriately determined and the model simulations were successful in representing the actual root system morphologies obtained by the experiment.

Similar to Figure 11, we divided each square (30 × 30 cm) shown in Figure 12c into 144 sub-squares (2.5 × 2.5 cm), and calculated the root length in each sub-square, recorded in the simulation. By dividing the root length by area of the sub-square, we obtained the root length density and show the distribution of the root length density in Figure 13. In Figure 13a, the roots concentrated at the central point of water supply more intensely than the observed root system (Figure 11a). However, the general shapes of the simulated root length distributions in both root boxes, shown in Figure 13, are in good agreement with observed distributions of root length density (Figure 11).

Discussion

To examine the reproducibility of the morphological architecture of a soybean root system through the experimental methods, we grew two more soybeans in root box No. 3 and No. 4. The size of the root boxes, the method of water supply, and the growth periods were the same as in root boxes 1 and 2, but the TDR probes were not installed into root box No. 3 and No. 4. Figure 14a, b shows the observed root system architecture that developed in root box No. 3 and 4. The total root length density in root box No. 3 and 4 are slightly higher than those in root box No. 1 and 2. Each individual root elongation is also different from the other. However, the morphological architectures of the entire root systems developed in root box No. 3 and 4, that is, root concentration, and the root deflection toward the point of water supply, are very similar to those in root box No. 1 and 2. By comparing these two sets of root systems, it can be said that the root system architecture affected by the water supply shown in Figures 10 and 11 are not special cases, but are representative of general soybean root systems. Therefore, we may regard root system No. 1 and No. 2 as representative of soybean root systems.

In this experiment, we set the root boxes horizontally for the purpose of reducing the effect of gravity on both the soil water flow and root system development. It is, however, impossible to eliminate the effect of gravity completely. During the experiment, it was observed that the main root and first order lateral roots responded to gravity deflecting downward, and then reached the bottom plate. After reaching the bottom plate, the roots changed their orientations and elongated parallel to the plate. The roots that branched from those already touching the bottom plate elongated parallel to the plate from the beginning. As a result, root elonga-

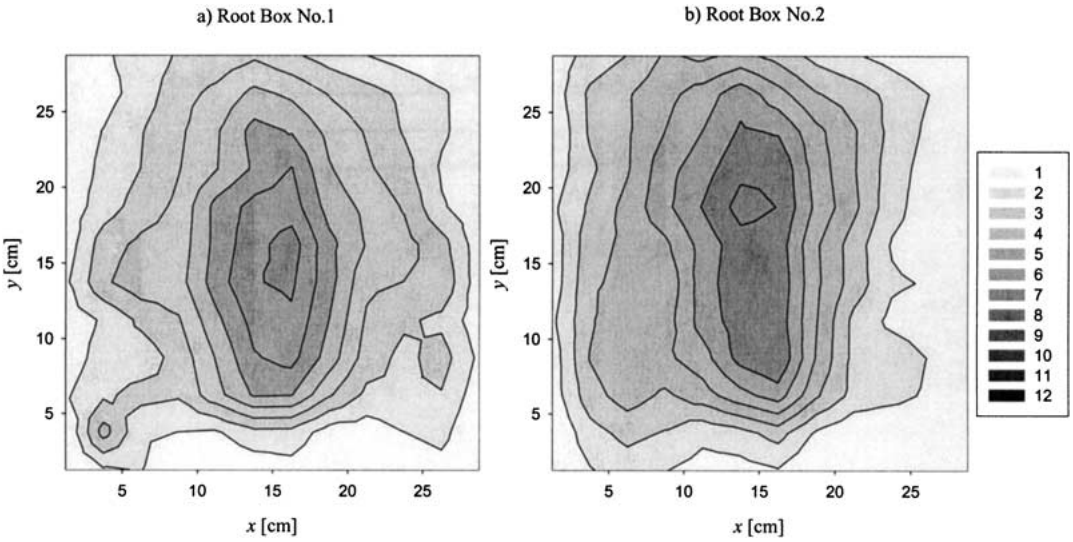

Figure 16. Distributions of root length density [cm/cm^2] in the root box (**a**) No. 1 and (**b**) No. 2, simulated without the effect of hydrotropism. The concentration of the root length to the points of water supply cannot be seen. (The figures correspond to the root systems shown in Figure 15.)

tion was exposed to the combined effects of gravity, touching the plate and water flow. However, it was observed that although the sectional shape of a root that touched the plate was distorted as it grew, the elongation zone of roots close to the root tip did not stick to the plate completely and their sectional shapes were not distorted. Also, sufficient growth of the entire root system was actually observed, and the plate and gravity seemed to have no harmful effect on the root elongation. Therefore, we suggested that the effect of touching the plate, ''thigmotropism'', might cancel out the effect of gravity ''gravitropism'', and that it is not necessary to consider this reduced effect of gravity on root system development. On the other hand, the difference of water potential between soil on the upper and lower plate was 2 cm, and the maximum difference of water content was 0.007 cm^3/cm^3. This value was obtained from the retention curve shown in Figure 6a. Therefore, we assumed that the differences in the water condition due to the thickness of the root box were also negligible. Moreover, due to the maximum water potential of −25 cm at the porous cups (see subsection ''Root box'' and Figure 3), the soil was not saturated, and no ''hypoxic area'' was produced in the root boxes throughout the experiment. This can also be confirmed from Figure 9.

It is possible that compensatory growth alone can account for root concentration at the points of water supply, and that the root hydrotropic response used in the present model is not necessary to represent the effect of soil water on root system development. To demonstrate the effect of root hydrotropism in the model, another pattern of root system development was simulated, that is, root system development with only compensatory growth, where root hydrotropism does not affect root elongation (k_h = 0.0, a_e= 40, ψ_e = −250 cm). This pattern is similar to that simulated in the model by Clausnitzer and Hopmans (1994), in the sense that the increasing resistance of root elongation is due to the decreasing soil moisture. Although soil resistance affected the direction of root elongation in the model by Clausnitzer and Hopmans (1994), root orientation does not, however, change in this simulation pattern. Figure 15 shows the root system architecture at the end of the growth period, simulated only with the effect of compensatory growth. In Figure 15a, b, roots elongate straight and do not change their direction of growth. The root length density seems to be slightly higher near the points of water supply. However, the concentrations of the roots to the point of water supply, which were seen in the actual root systems in root boxes, cannot be seen in these results. The higher water content around the porous cups in Figure 15 than in Figure 9c also indicates that the concentration of roots to the points of water supply is not enough. To confirm this result quantitatively, the distribution of the root length density is shown in Figure 16. In Figure 16 also, the concentration of roots at the points of water supply is not sufficient when compared to those in Figures 11 and 13. And the distribution of root length density in Figure 16a and b is quite similar. Although we repeated the simulations with different values of parameters (a_e, ψ_e), we could not

obtain the root system architectures similar to those in Figure 10.

These results indicate that the effect of compensatory growth only cannot demonstrate the effect of soil water on root system development, and that a factor that changes the direction of root elongation due to the effect of soil water is necessary. Therefore, root hydrotropism, which was the effect used to change the direction of root elongation in the model, is an irreplaceable factor for representing the effect of soil water flow on root system development. Because the root branching interval was assumed to be constant in the model, there still remains the possibility that compensatory growth with changing branching intervals represents root concentration to the points of water supply. In any event, without an effect such as hydrotropism that changes the direction of root elongation, the model cannot simulate root deflection toward the point of water supply or elongation away from the point of water supply, as described above.

As we have seen, the simulated root system architectures (Figure 12c) are in good agreement with the observed actual root system architectures (Figure 10), and the changes in distribution of the soil water content (Figure 12) are also in good agreement with those obtained by TDR measurements in the experiment (Figure 9). These results confirm that the combined model of root system development and soil water flow used in this study successfully simulated root system development under different environmental soil water conditions, and that hydrotropism and the compensatory growth of roots are the dominant factors in root system development under a reduced effect of gravity.

Conclusion

Through plant root system growth experiments under a reduced effect of gravity, it was clarified that root system development was controlled by the soil water flow, that is, the roots tend to grow towards the direction of the water supply and concentrate in areas around the points of water supply. These effects of soil water conditions on root system development seem to be caused by hydrotropism and compensatory growth of roots. We successfully simulated root system development and soil water flow by a model considering both root hydrotropism and compensatory growth. The observed and simulated root system morphological architectures, and the measured and simulated changes of distribution of soil water content were in good agreement quantitatively. Consequently, the hypothesis that root hydrotropism is the dominant factor in root system development in the case of a reduced effect of gravity was confirmed. Also, the observations and simulations of the root system development in the root boxes suggested the importance of root compensatory growth in root system development. It was confirmed that compensatory growth alone, however, cannot account for the root concentration to the points of water supply seen in the experiment.

The combined model of root system development and soil water flow, considering root hydrotropism and the compensatory growth used in this study, can simulate and predict root system development under various soil water conditions. The model can be applied to design and control root system architecture under the influence of drip irrigation. Furthermore, the model can provide important information on how to control root system development under reduced gravity conditions, that is, plant growth in a space station.

In this study, a two-dimensional model was used to simulate root system development and soil water flow because the root box experiment may be regarded as two-dimensional. However, it is necessary to extend the model into a three-dimensional set to simulate practical root system development under field conditions.

References

Clausnitzer V, Hopmans JW. 1994. Simultaneous modeling of transient three-dimensional root growth and soil water flow. Plant and Soil 164:299–314.

Crossett RN, Campbell DJ, Stewart HE. 1975. Compensatory growth in cereal root systems. Plant and Soil 42:673–683.

Darwin C. 1880. The power of movement in plants. London: John Murray.

Diggle AJ. 1988. ROOTMAP—a model in three-dimensional coordinates of the growth and structure of fibrous root systems. Plant and Soil 105:169–178.

Dutrochet H. 1824. Physiologische Untrsuchungen uber die Beweglichkeit der Pflanzen. Ubersetzt von Nathansohn. Ostwald's Klassiker der exacten Wissenschaften, 144 Cited by von Sachs (1887).

Galamay TO, Yamauchi A, Nonoyama T, Kono Y. 1992. Acropetal lignification in protective tissues of cereal nodal root axes as affected by different soil moisture conditions. Jpn J Crop Sci 61(3):511–517.

Herkelrath WN, Miller EE, Gardner WR. 1977. Water uptake by Plants: II. The root contact model. Soil Sci Soc Am J 41:1039–1043.

Hooker Jr HD. 1915. Hydrotropism in roots of *Lupinus albus*. Ann Bot 29:265–283.

Ishikawa H, Hasenstein KH, Evans ML. 1991. Computer-based video digitizer analysis of surface extension in maize roots. Planta 183:381–390.

Istoke J. 1989. Grandwater modeling by the finite element method. Washington, DC: American Geophysical Union, p 495.

Jourdan C, Rey H. 1997. Modeling and simulation of the architecture and development of the oil-palm (*Elaeis guineensis* Jacq.) root system I. The model. Plant Soil 190:217–233.

Kanda M, Hino M. 1990. Numerical simulation of soil-plant-air system (1) modeling of plant system. J Japan Soc Hydrol Water Resour 3:37–46 (in Japanese with English summary).

Keith P. 1815. On the development of the seminal germ. Trans Linn Soc 11:252–269.

Kono Y, Yamauchi A, Nonoyama T, Tatsumi J, Kawamura N. 1987. A revised experimental system of root-soil interaction for laboratory work. Environ Control Biol 25(4):41–151.

Kosugi K. 1996. Lognormal distribution model for unsaturated soil hydraulic properties. Water Resour Res 32:2697–2703.

Lynch J, van Been JJ. 1993. Growth and architecture of seedling roots of common bean genotypes. Crop Sci 33:1253–1257.

Lynch JP, Nielsen KL, Davis RD, Jablokow AG. 1997. SimRoot: modelling and visualization of root systems. Plant Soil 188:139–151.

Morita S, Toyota M. 1998. Root system morphology of pepper and melon at harvest stage grown with drip irrigation under desert conditions. Jpn J Crop Sci 67(3):53–357 (in Japanese with English summary).

Nissen HH, Moldrup P, Henriksen K. 1998. High-resolution time domain reflectometry coil probe for measuring soil water content. Soil Sci Soc Am J 62:1203–1211.

Pages L, Jordan MO, Picard D. 1989. A simulation model of the three-dimensional architecture of the maize root system. Plant Soil 119:147–154.

Raper Jr CD, Barber SA. 1970. Rooting system of soybeans. I. Difference in root morphology among varieties. Agron J 62:581–584.

Shibusawa S. 1994. Modelling the branching growth fractal pattern of the maize root system. Plant Soil 165:339–347.

Somma F, Hopmans JW, Clausnitzer V. 1998. Transient three-dimensional modeling of soil water and solute transport with simultaneous root growth, root water and nutrient uptake. Plant Soil 202:281–293.

Takahashi H. 1994. Hydrotropism and its interaction with gravitropism in roots. Plant Soil 165:301–308.

Takahashi H, Scott TK. 1993. Intensity of hydrostimulation for the induction of root hydrotropism and its sensing by the root cap. Plant Cell Environ 16:99–103.

Takano M, Takahashi H, Hirasawa T, Suge H. 1995. Hydrotropism in roots: sensing of a gradient in water potential by the root cap. Planta 197:410–413.

Tsutsumi D, Kosugi K, Mizuyama T. 2001. Application of root system development model assuming the tropisms for seedling in Japanese red pine (*Pinus densiflora*). J Jpn Soc Reveget Tech 26(4):309–319 (in Japanese with English summary).

Tsutsumi D, Kosugi K, Mizuyama T. 2002. Observation of 2- dimensional root system development and soil water distribution in root boxes. For Res Kyoto 74:99–109 (in Japanese with English summary).

Tsutsumi D, Kosugi K, Mizuyama T. 2003. Root system development and water extraction model considering hydrotropism. Soil Sci Soc Am J 67:387–401.

Vaz CPM, Hopmans JW. 2001. Simultaneous measurement of soil penetration resistance and water content with a combined penetrometer-TDR moisture probe. Soil Sci Soc Am J 65: 4–12.

Zienkiewicz OC. 1971. The finite element method in engineering science. Berkshire: McGraw-Hill, p 575.